Third International Conference on CFD in the Minerals and Process Industries
CSIRO, Melbourne, Australia
10-12 December 2003

CFD ANALYSIS INVOLVING LIQUID ALUMINIUM IN-FURNACE CLEANING PROCESS

Jin L. SONG[1], Mark R. JOLLY[1], Mitsumasa KIMATA[2], Waldemar BUJALSKI[3] and Alvin W. NIENOW[3]

[1]Interdisciplinary Research Centre, School of Engineering, The University of Birmingham. Edgbaston, Birmingham, B15 2TT, U.K.

[2] Department of Chemistry and Chemical Engineering, Yamagata University 4-3-16 Japan, Yonezawa 992-8510, JAPAN

[3]Department of Chemical Engineering, School of Engineering, The University of Birmingham, Edgbaston, Birmingham, B15 2TT, U.K.

ABSTRACT

A chlorine/inert gas mixture is widely used for cleaning liquid aluminium by fluxing. However the potential leakage of chlorine and chemical reaction product hydrogen chloride gas is considered to be dangerous to society and faces the restriction in the new clean air regulations. Alternative fluxing methods, which have the same or superior cleaning effect, are necessary for the aluminium production industry. One of the techniques developed in the last ten years is the injection of granules of solid halides with mechanical agitation through an impeller or a lance. The purpose of the present project is to understand underlying science of the fluxing process through laboratory physical modelling and CFD simulation. It is found that at equivalent mean specific energy dissipation rates, mechanical agitation process through impeller should have better fluxing quality than lance bubbling process.

NOMENCLATURE

D	Impeller diameter
g	Gravitational constant
N	Rotation speed of impeller
M	Torque
P	Power
Po	Power number
V	Volume of fluid
v_S	Superficial gas velocity
ρ_L	Liquid density
$\overline{\varepsilon}_T$	Mean specific energy dissipation rate

INTRODUCTION

The demand of aerospace and automobile industry has caused aluminium production to grow by an annual average of around 4% for the last decade or so. In order to meet the ever increasing requirement for mechanical properties, continuous improvements in the melt treatment process is necessary (Peterson et al. 1995; Waite, 2002). Generally speaking there are certain elements in the molten aluminium which are detrimental to its quality (Simensen and Nilmani, 1995), for example, alkalis (sodium, calcium, lithium) causing edge cracking in aluminium sheet production (Williams, 2001), and excess hydrogen causing porosity formation during solidification (Stevens and Yu, 1986). Traditionally chlorine/inert gas mixture was injected into the liquid aluminium through static lance, steel wands and porous plug. However this process generates large gas bubbles, which are distributed in the melt. This results in ineffective mass transfer and reaction and therefore poor utilization of chlorine gas. Such bubbling is also required to provide the motive power for mixing the aluminium and this too is very inefficient. To compensate for the inefficiency of furnace fluxing, excess chlorine gas is used, which leads to high production cost and gives rise to a potentially severe environmental issue as it leaves the reactor. Over the last five years or so, reducing or eliminating the use of chlorine gas in the holding furnace has become the top priority for most aluminium producing companies (Flisakowski et al. 2001). This can be achieved by the introduction of Rotary gas/salt Fluxing Technology (RGI/RFI rotary fluxing injection) (Bilodeau et al. 2001). The industrial implementation of the rotary gas/salt fluxing technology has proven to be a metallurgical and environmental benefit to the traditional chlorine fluxing process in terms of the emission requirements and removal efficiency of dissoluted hydrogen, alkali metals, and inclusions found in molten aluminium metals (Flisakowski et al. 2001). Because the rotary impeller ensures an efficient break-up of the gas bubbles and salt injected in its vicinity (reaction zone), and provides global metal circulation, which makes it the most efficient fluxing method in furnaces. In terms of environment and safety, the most important potential benefit is the replacement of chlorine gas by salt fluxes, which greatly reduced atmospheric emissions of HCl, Cl_2, and dust. In this research, by carrying out physical model and CFD simulation, the velocities measured using PIV (particle image velocimetry) are compared with those predicted from CFD simulation for both single lance bubbling and mechanical agitation process. The results illustrated clearly that RGI/RFI mechanical agitation fluxing is superior to gas bubbling process.

THE SETTING-UP OF PHYSICAL MODEL

The industrial melting furnace is normally large and shallow. For the physical model in the present research, a water tank (length 650 mm, width 254 mm, and height 130 mm), which is scaled down by a linear factor of 10 compared to a typical industrial furnace, was set up for both lance bubbling and mechanical agitation system (Figure 1). Water was chosen as the fluid because its kinematic viscosity is similar to that of liquid aluminium (Chen et al, 2001). Air was assumed to be the best way of modelling the chlorine gas (or its diluted mixture with nitrogen/argon) (Carpenter and Hanagan, 2001).

For the lance bubbling process, the air was introduced through a single lance (a glass tube with a bore of 1 mm) positioned in the centre line (y=0) at a chosen angle to the base with the end positioned about z=10 mm from the

bottom and x=200 mm from one end of the longest dimension. For the mechanical agitation process, the impeller was positioned at a similar place as the lance, i.e. at a particular entry angle with the middle of the end the shaft positioned at z=20 mm and x=200 mm from one end of the tank. Particle image velocimetry (PIV) was used to obtain instantaneous liquid velocity, in which the water is seeded with small(~10μm) buoyant particles and illuminated with a plane sheet of laser light. As the particles have nearly the same density as water, they act as flow followers in the local transient velocity field without disturbing the flow itself. The transient flow pattern of the liquid within the light sheet is calculated from the displacement of the particles between successive images of the flow field (Gray and Greated, 1987).

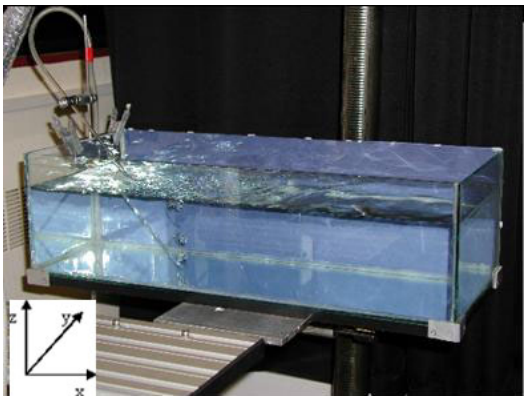

Figure 1: Water tank used for lance bubbling and mechanical agitation.

In order to compare the effectiveness of mixing between the lance bubbling and the mechanical agitation process, mean specific energy dissipation rates, $\overline{\varepsilon}_T$, parameter was chosen to link the two process. In the case of gas bubbling, the full thermodynamic relationship for $\overline{\varepsilon}_T$ can be simplified for shallow liquids (Boswell et al, 2003) to give formula (1):

$$\overline{\varepsilon}_T = g v_S \rho_L \qquad (1)$$

For the case of the mechanical agitation, it is estimated by the formula (2):

$$\overline{\varepsilon}_T = \frac{Po \rho_L N^3 D^5}{V} \qquad (2)$$

In the present research, the volumetric flow rate has also been scaled down based on the industrial operation data, the lower and higher volumetric flow rates are 0.1 l/min and 1.0 l/min. Based on the above formula, for the same mean specific energy dissipation rates, the equivalent impeller rotation speeds are 162 and 348 rpm respectively (Kimata et al, 2003).

SIMULATION RESULTS AND DISCUSSION

A number of CFD commercial software packages are available to model this phenomenon. In the present investigation, Flow-3D is chosen to model lance bubbling process and CFX5.5 is used for mechanical agitation process. Both codes used Navier-Stokes equations to describe fluid flow.

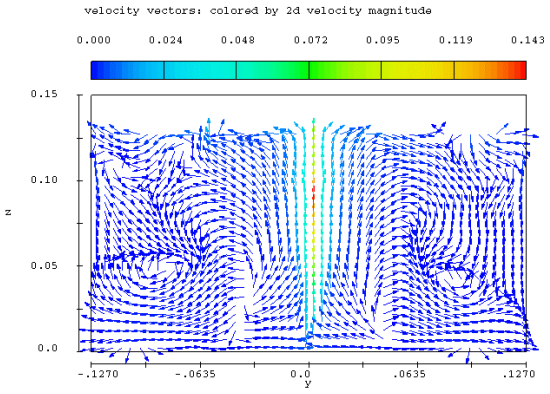

Figure 2: Velocity vector plot from CFD of cross plane near lance position at volumetric flow rate 0.1 l/min.

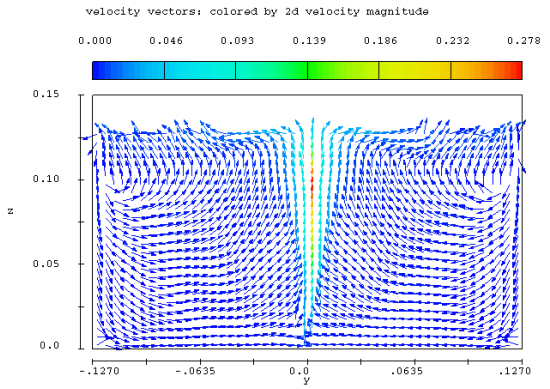

Figure 3: Velocity vector plot from CFD of cross plane near lance position at volumetric flow rate 1.0 l/min.

Gas Bubbling Process

In order to model coalescence and break-up of moving bubbles, at least three cells in each direction are needed for each bubble. However with present tank is 650 mm long, and the bubble size of 2-7 mm diameter, the computational cost will be extremely high. However alternatively in Flow-3D, a particle model can be used to simulate bubble behaviour, in which the particles can have the properties of an air bubble and interact with the liquid. The model does not require the use of surface tension or fine grids. The source of the particles was chosen at exactly the same position as that in the physical model. Based on the experimental observations, the bubble size is defined by five groups which vary from 5 mm to 10 mm. In the model, equal volume fractions of the bubble sizes were used to induce flow and turbulence, but they do not coalesce or break up. Figure 2, 3 show the velocity vector plots at cross plane near lance position at volumetric flow rate 0.1 and 1.0 l/min. It can be found that the flow patterns are more or less the same, in which high velocity occurred at the centre of the cross section. The maximum velocity is 0.143 m/s at the volumetric flow rate 0.1 l/min, and 0.278 m/s at the volumetric flow rate 1.0 l/min. It would be understandable that with the increasing volumetric flow rate, more air bubbles will flow up to the water surface, and the water velocity at the vertical direction would be higher. At low volumetric flow rate, some recirculation occurred at the bottom half of the cross section, and at high volumetric flow rate the recirculation

happened at the top half of the cross section. Figure 4 shows the PIV measured result at the same cross section under the volumetric flow rate 1.0 l/min. The maximum velocity is 0.15 m/s. Comparing with the results from Figure 3, it can be found that the flow patterns are quite similar, and the predicted maximum value is slightly higher than PIV measurement. This could be explained as follows: PIV cannot catch water velocity at the bubble surface because of focusing problem, the velocity there is happened to be the maximum one. However CFD can predict the velocity near the bubble, so there is a discrepancy between predicted and measured maximum velocity. Because the air was introduced by a single lance, the velocity at both ends of the tank will be much smaller than that at the position of the lance. This can be found in Figure 5, in which the maximum velocity is only 0.0385 m/s at volumetric flow rate 1.0l/min.

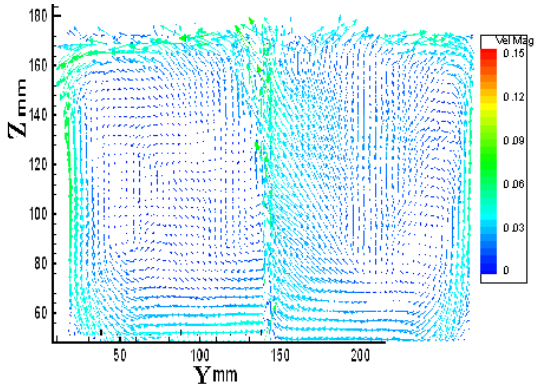

Figure 4: PIV measured velocity vectors plot for cross plane near lance position at volumetric gas flow rate of 1.0 l/min.

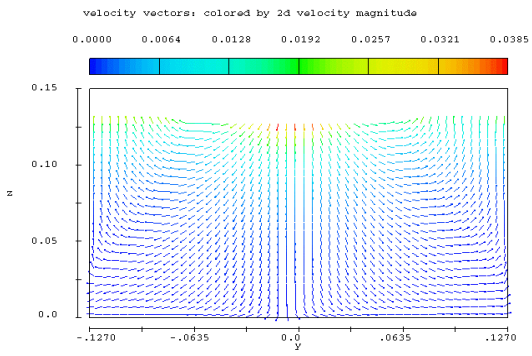

Figure 5: Velocity vector plot from CFD at plane 10 mm to the edge of the tank at volumetric flow rate 1.0 l/min.

During aluminium refining it is essential to have good mixing for efficient mass transfer and rapid chemical reaction. Comparing the velocity profile in Figure 3 & 5, even though the maximum velocity is 0.278 m/s at the cross section near lance position, the maximum velocity at the far end of tank is only 0.0385 m/s, and the most of the bottom half cross section is nearly zero. Changing the lance angle gave limited improvement about the velocity field. Figure 6 shows the predicted maximum cross section velocity at the lance position with different lance angles at volumetric flow rate 1.0 l/min. It seemed that the lance angle between 45° and 60° have a better maximum velocity, but does not show substantial increases. Other improvement methods include more lances and porous plug.

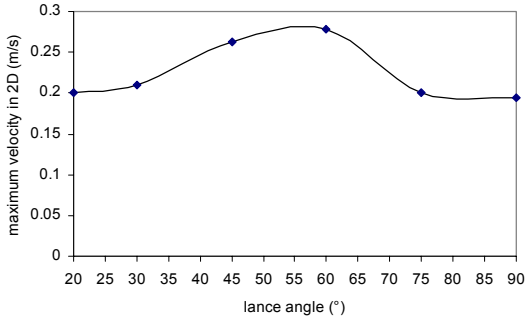

Figure 6: Max. predicted water rising velocity changing with lance angles at volumetric flow rate 1.0 l/min.

The porous plug is intended to produce small bubbles. But the experiments confirm that the small bubbles might quickly coalescence and generate large bubbles depending on the liquid purity (Clift et al, 1978). In practice, the difficulty is overcome by changing the position of the lance throughout the refining process. This is not a very well controlled and this can lead to variable results.

Mechanical Agitation

Different types and geometries impeller could be chosen in order to replace lance bubbling process. The basic principle here is to choose a simple design and particular attention is paid to achieve a high power input and hence good fluid motion and mixing without swirling on the top surface, which is highly undesirable in aluminium fluxing process as the swirling could bring the dross on the top surface into the liquid and produce further impurities or inclusions. After a series of laboratory tests, a three bladed (30 deg pitch) turbine downwards pumping (3PBT30) with a measured power number, Po=0.44, in Figure 7, was selected.

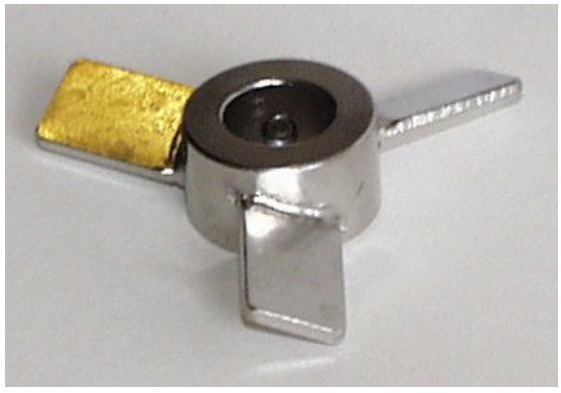

Figure 7: The impeller studied (3PBT30; D=48mm)

In order to investigate the optimum position of the impeller, the impeller shaft could be arranged at different entry angles relative to the top surface of the tank. Generally speaking, two methods (multiple frame of reference or MFR, and sliding mesh model) can be used to deal with the impeller rotation phenomenon. However, as the sliding mesh method requires much longer CPU time an MFR (Sandhu and Foumeny, 1996), in present research MFR technique is used to model the rotation of the impeller. There are two domains in the model; one is the

rotating domain around the impeller, and the other is the rectangular tank. Frozen rotor frames change model is applied to the unmatched interface between the two domains, which provides a "steady state" solution to the multiple frames of reference problems. k-ε turbulence model was used for obtaining velocity fields in the system (CFX-5.5 Solver, 2002). The governing differential equations were discretised and solved using a finite volume technique (Versteeg and Malalasekera, 1989). In order to validate the CFD model, power number predicted from CFD model is compared with that measured from experiment. Because the impeller power number can only be measured with impeller shaft at 90° to the surface, CFD model was also set up exactly the same as experiment. The predicted torque is 0.000137 Nm. According to formulae 3 and 4,

$$P = 2\pi NM \tag{3}$$

$$Po = \frac{P}{\rho_L N^3 D^5} \tag{4}$$

the predicted power number for present three turbine bladed impeller is 0.47, which is close to the measured data 0.44.

Figure 8 shows the pressure distribution in the vertical plane for the domain of impeller at impeller rotation speed 162 rpm.

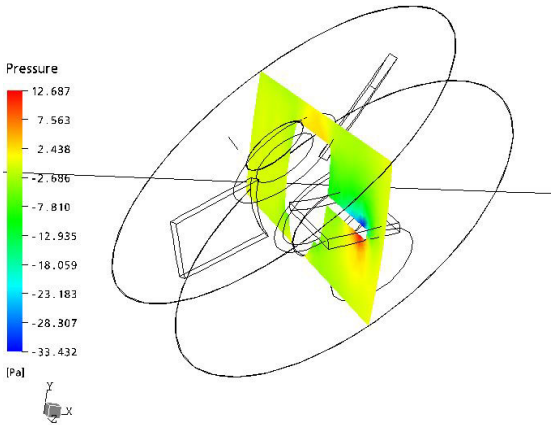

Figure 8: Pressure distribution from CFD around the blade at rotation speed of 162 rpm.

It can be found that below the blade a quite high pressure is building up, while above the blade there is a negative pressure, which is quite reasonable if the impeller rotates clockwise. Figure 9 and 10 show the vertical velocity contour line plot at both ends of the tank and near impeller blade for low (162 rpm) and high (348 rpm) rotation speeds. As mentioned early, the reason for choosing 162 and 348 rpm is to have the equivalent mean specific energy dissipation rate as the lance bubbling process. It can be seen that the maximum upward and downward speeds are 0.237 and -0.174 m/s (using "-" sign convention for downwards) at the high rotation speed 348 rpm, and 0.097 and -0.118 m/s at the low rotation speed 162 rpm at cross section near impeller blade. Since the flow patterns in Figures 2, 3 and Figures 9, 10 are different, it is difficult to compare velocity directly, but the range of the values is quite similar. The CFD predicted result was also compared with PIV measured data, which is shown in Figure 11.

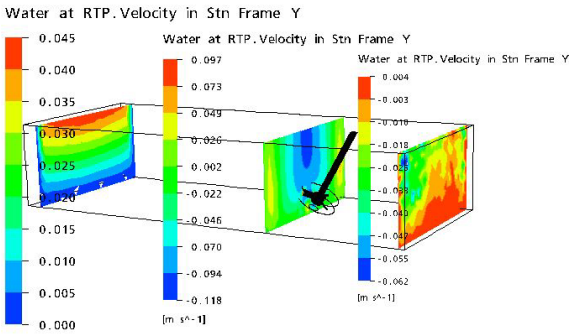

Figure 9: Velocity contour plot from CFD of cross sections at both ends of the tank and near impeller blade for rotation speed of 162 rpm (angle 60°; view reversed compared to Figure 1, i.e. x=0 is RHS).

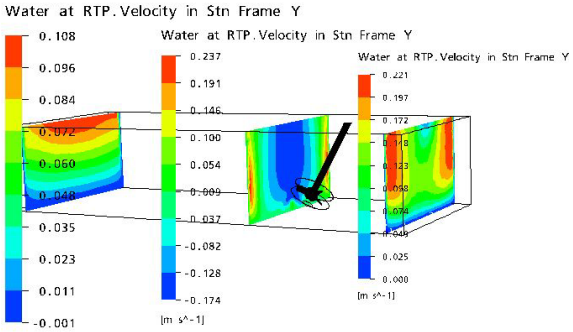

Figure 10: Velocity contour plot from CFD of cross sections at both ends of the tank and near impeller blade for rotation speed of 348 rpm (angle 60°; view reversed compared to Figure 1, i.e. x=0 is RHS).

Comparing cross section velocity profile near impeller blade position in Figure 10 and 11, it can be found that the flow pattern is quite similar, i.e. the middle part is going down and the both sides rising up. The downward velocity predicted from CFX5.5 is 0.174 m/s, and the velocity measured from PIV is 0.15 m/s, which shows reasonable agreement.

In order to find the optimum entry angle for the impeller shaft, simulations were carried out with different shaft entry angles. Figures 12, 13, 14, and 15 show the contour line velocity plots near impeller blade for different entry angles, and the Table 1 shows the vertical velocities at different cross sections.

Entry angle	Near blade x≅220 mm (m/s)		Left side x≅0 mm (m/s)		Right side x≅650 mm (m/s)	
(°)	up	down	up	down	up	down
30	0.16	-0.14	0.30	-1.53	0.53	0
45	0.09	-0.20	0.02	-0.16	0.10	0
60	0.24	-0.17	0.22	-0.00	0.11	0
75	0.05	-0.11	0.02	-0.07	0.03	0

Table 1: Vertical velocities of water from CFD result at different planes for mechanical agitation with impeller rotation speed of 348 rpm.

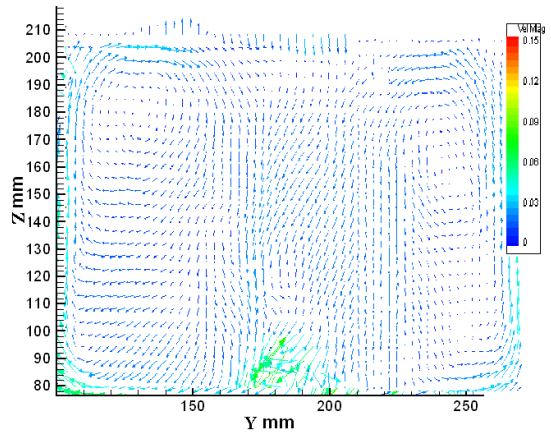

Figure 11: PIV measured data for 3PBT30 at rotating speed 348 rpm and an entry angle of 45°.

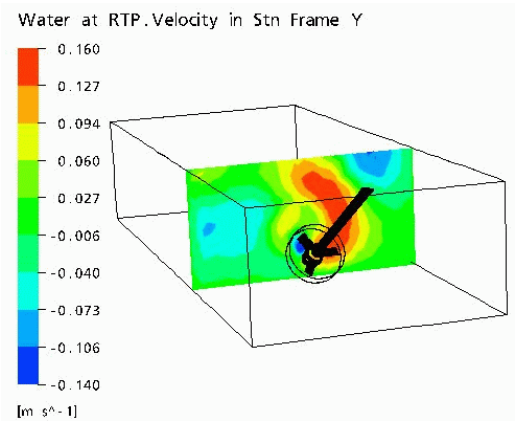

Figure 12: Velocity contour plot from CFD near impeller blade at entry angle 30° (348 rpm).

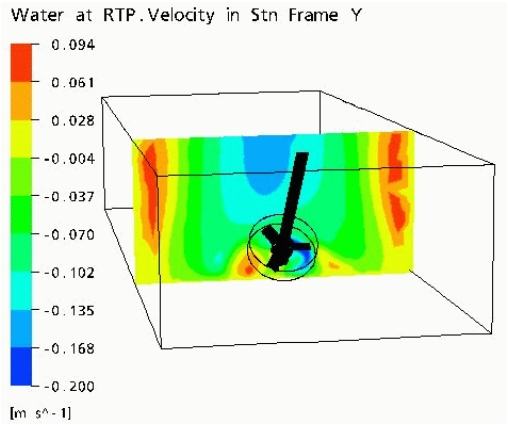

Figure 13: Velocity contour plot from CFD near impeller blade at entry angle 45° (348 rpm).

At entry angle 30°, the higher velocity area is in the bottom half of the tank, which is not ideal for fluxing process. There are similar flow patterns for entry angles at 45° and 60°, in which the middle part goes down and the both sides rise up, which would be ideal for chemical reaction products to float up to the surface. At entry angle 75°, velocity is found smaller than those at 45° and 60° situation. So it can be concluded that an entry at about 45° to 60° should have better fluxing. Perhaps entry angle 60 is the optimum angle according to the data from Table 1.

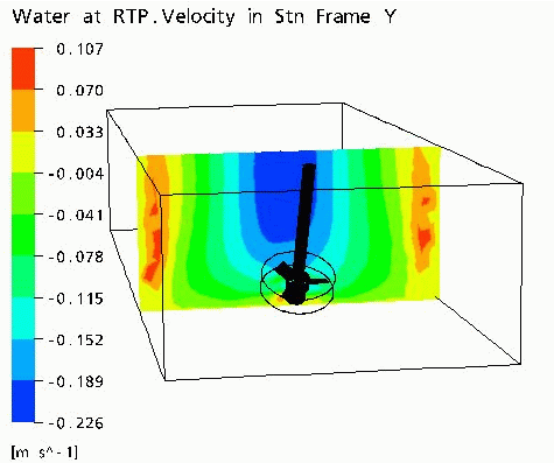

Figure 14: Velocity contour plot near impeller blade at entry angle 60° (348 rpm).

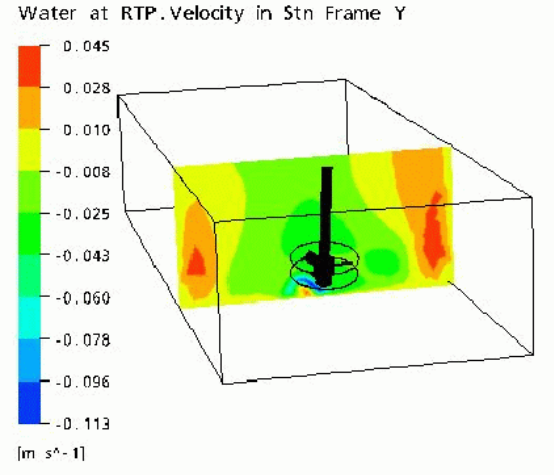

Figure 15: Velocity contour plot near impeller blade at entry angle 75°(348 rpm).

This maybe related to the geometry of the tank, and more investigation need to be done into the relationship between impeller entry angle and tank geometry.

EXPERIMENTAL ASSESSMENT OF MIXING/HOMOGENISATION EFFICIENCY

It would be difficult to judge which process is superior to the other just from the velocity distribution in the water tank. As revealed in Figures 2, 3, 9, and 10, the velocity pattern is totally different for gas bubbling compared to mechanical agitation. With gas bubbling, in cross section, the middle part is rising up, and there are two circulations on each side. With mechanical agitation, in cross section, the middle part is actually going down, and water at both edges is rising up. In order to compare the mixing efficiency of gas bubbling versus mechanical agitation, decolourization experiments were carried out, in which sodium thiosulphate is added to starch/iodine solutions (Cronin and Nienow, 1994). Figure 16 shows mixing time for both lance bubbling at 1.0 l/min and 3PBT30 impeller at 348 rpm. It can be seen that the mixing time from 3PBT30 impeller is much shorter than that from lance

bubbling process, and the mixing time in the case of mechanical agitation is less dependent on the position of the reactant addition point.

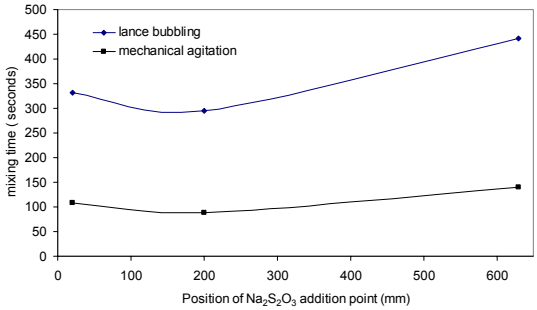

Figure 16: Mixing time for lance bubbling (volumetric flow rate 1,0 l/min) and mechanical agitation (rotation speed 348 rpm) at 45° as a function of addition position of the tracer.

This could be explained from the velocity profile in Figures 5 and 10, in which the lance bubbling and mechanical agitation processes have the equivalent mean specific energy dissipation rate, the velocity at the far end of the tank in the case of mechanical agitation (as obtained from CFD simulations) is at least three times higher than that for the case of lance bubbling, which will reduce mixing time significantly.

CONCLUSIONS

Both gas bubbling and mechanical agitation process have been tested in a scaled down water tank and CFD simulation. The velocity patterns from both CFD simulation and PIV under different conditions have been fully compared. Generally there is a reasonable agreement between predicted velocities and measured values. In the case of lance bubbling, even though there is a high velocity field near lance area, the velocity at both ends of the tank is small, and changing the lance angle does not improve the velocity distribution significantly. In the case of mechanical agitation through impeller, at the same mean specific energy dissipation rate, $\overline{\varepsilon}_T$, as in the case of lance bubbling process, the velocity at both ends of the tank increased about three times. The mixing time of mechanical agitation through impeller is much lower than that for the lance bubbling process, so a better fluxing result could be expected.

ACKNOWLEDGMENTS

The authors, JLS and WB, would like to acknowledge the financial support from EPSRC for the project "Physical and computational modelling of non-chlorine cleaning of aluminium in furnace as a tool for cleaning process design". Thanks are also given to our industrial partners, N-Tec, MQP/STAS, VAW, Norton Aluminium, Carney Ltd, and Alba, for both financial and technical support to this project. Technical help from Mr R. Sharpe is also acknowledged.

REFERENCES

BILODEAN, J.F., LAKRONI, C., KOCAEFE, Y., (2001), "Modelling of rotary injection process for molten aluminium processing", *Light Metals 2001*, TMS (The Minerals, Metals & Materials Society), 1009-1015.

BOSWELL, C.D., VARLEY, J., BOON, L., HEWITT, C.J., NIENOW, A.W., (2003), "Studies on the impact of mixing in brewing fermentation - Comparison of methods of effecting enhanced liquid circulation", *Food and Bioproducts Processing*, **81,** 33 - 39.

CARPENTER, K.A., and HANAGAN, M.J. (2001), "Efficiency modelling of rotary degasser head configurations and gas introduction methods, aprt1-water tank tests", *Light Metals 2001*, TMS(The Minerals, Metals & Materials Society), 1017 - 1020.

CHEN, J.J.J., ZHAO, J.C., LACEY, P., GRAY, T., (2001), "Flow pattern detection in a melt treatment water model based on shaft power measurements", *Light Metals 2001*, TMS (The Minerals, Metals & Materials Society), 1021-1025.

CFX-5.5 SOLVER, (2002), AEA Technology Engineering Software, 279 – 280.

CLIFT, R., GRACE, J.R., WEBER, M.E., (1978), "Bubbles, drops and particles", *Academic Press, Inc(London) Ltd.*

CRONIN, D.G., NIENOW, A.W., MOODY, G.W., (1994), "*Food Bioproducts Processing, Trans IChemE (Part C),* **72,** 35 - 40.

FLISAKOWSKI, P.J., MCCOLLUM, J.M., FRANK, R.A., (2001), "Improvements in Cast Shop Processing Using Pyrotek's HD-2000 and PHD-50 Rotary Injector System", *Light Metals 2001*, TMS (The Minerals, Metals & Materials Society), 1041 - 1047.

GRAY, C., GREATED, C.A., (1987), "The application of particles image velocimetry to study of water wave", *Optics and laser in engineering*, **9,** 265 - 276

KIMATA, M., NAYAN, N., BUJALSKI, W., NIENOW, A.W., SONG, J.L., JOLLY, M.R., (2003), "Mixing studies related to the cleaning of molten aluminium", *Proc. 11th European Mixing Conference 2003, Bamberg, 14-17 October 2003 (accepted).*

PETERSON, R.D., WELLS, P.A., CREEL, J.M., (1995), "Reducing chlorine usage in furnace fluxing: two case studies", *Light Metals 1995*, TMS (The Minerals, Metals & Materials Society), 1197 - 1202.

SANDHU, K.S., FOUMENY, E.A. (1996), "Turbulence modelling of the fluid dynamics in fully baffled stirred vessels", *The 1996 IChenE Research Event, The University of Leeds*, **Vol. 2**, 877 – 879.

SIMENSEN, C.J., NILMANI, M., (1996), "A computer model for alkali removal from molten aluminium", *Light Metals 1996*, TMS (The Minerals, Metals & Materials Society), 995 - 1000.

STEVEN, J.G., YU, H., (1986), "Mechanism of sodium, calcium and hydrogen removal from an aluminium melt in a stirred tank reactor – the ALCOA 622 process", *Light Metals 1988*, TMS (The Minerals, Metals & Materials Society, 437 - 443.

VERSTEEG, H.K., MALALASEKERA, W., (1989), "An introduction to computational fluid dynamics. The finite volume method", *Longman Scientific & Technical.*

WAITE, P., (2002), "A technical perspective on molten aluminium processing", *Light Metals 2002*, TMS (The Minerals, Metals & Materials Society), 841 – 848.

WILLIAMS, E.M., (2001), "Alkali removal and reduced chlorine use during furnace fluxing", *Light Metals 2001*, TMS (The Minerals, Metals & Materials Society), 1053 – 1059.